

## APPLICATION OF CLUTTER SUPPRESSION METHODS TO A GEOSTATIONARY WEATHER RADAR CONCEPT

S. L. Durden and S. Tanelli

Jet Propulsion Laboratory  
California Institute of Technology  
4800 Oak Grove Dr., Pasadena, CA 91109, USA

**Abstract**—While a geostationary weather radar would enable unprecedented monitoring of hurricanes and other severe weather, surface clutter could seriously limit its performance. The large incidence angles necessary for wide-area coverage, combined with the footprint size could cause surface clutter to obscure atmospheric return up to several km above the surface. The authors describe a Doppler filtering approach to clutter suppression and show simulation results. They find that Doppler filtering can significantly reduce the surface return, bringing surface clutter to acceptable levels. The authors then consider this approach when a staggered pulse repetition frequency is used to improve the maximum unambiguous velocity. They find that a method previously developed for ground-based weather radars can be successfully applied.

### 1. INTRODUCTION

Spaceborne radar observation of clouds and precipitation began with the launch of the Tropical Rainfall Measuring Mission (TRMM) in 1997 [1] and has continued with the launch of CloudSat in 2006 [2]. A variety of follow-on missions have been planned or recommended, including a conceptual design of a geostationary weather radar, dubbed “NEXRAD-in-Space” (NIS) [3]. A weather radar in geostationary orbit is highly desirable owing to its unique ability to simultaneously provide vertical rainfall profiles, wide spatial coverage, and frequent observations (e.g., hourly or better); these characteristics make it well-suited to operational monitoring of hurricanes and severe storms. One

---

Corresponding author: S. L. Durden (sdurden@jpl.nasa.gov).

of the many challenges in implementing such a radar is clutter from the surface, particularly at the large incidence angles required for good areal coverage from geostationary orbit. In this letter we provide a brief summary of the NIS design and an analysis of the clutter problem. We then present a solution using Doppler filtering with a staggered pulse repetition frequency (PRF).

## 2. NIS OVERVIEW AND CLUTTER PROBLEM

The NIS instrument is designed to measure reflectivity and Doppler velocity at 35 GHz from geostationary orbit at an altitude of about 36,000 km [3]. Table 1 shows the instrument characteristics. The instrument uses a spherical reflector antenna and mechanically scanned feed system with spherical aberration correction [4]. The spherical design was chosen so that the beam quality does not degrade with scan angle, as would be the case for a parabolic shape. The beam is scanned from  $0^\circ$  to  $4^\circ$  off-nadir to provide full coverage of a 5200 km circular area on the earth's surface. Because of the earth's curvature, a look angle of  $4^\circ$  off nadir results in an incidence angle of  $28^\circ$  relative to the earth's surface. With the planned 28-m aperture reflector (effective illuminated area for any given beam), the beam size is roughly 12 km. At  $28^\circ$  incidence the beam tilt results in an effective vertical resolution of nearly 6 km ( $12 \sin 28^\circ$ ). Hence, clutter from the earth's surface return could potentially affect the first 6 km above the surface at the edge of the scan. Since most liquid water is in the first five km, this presents a serious challenge in monitoring the full coverage area. The vertical extent of the surface clutter effect is reduced towards the center of the scan to the limit given by the actual shape of the radar's point

**Table 1.** Key NIS system parameters.

Frequency (GHz)	35.6
Range Resolution (m)	250
Horizontal Resolution (km)	12
Pulse Compression Sidelobes (dB)	-55
Pulse Length (microsec)	60
Bandwidth (MHz)	2
Sample Frequency (MHz)	10
Antenna Electrical Aperture (m)	28
Beamwidth (deg.)	0.02
Minimum Detectable Reflectivity (dBZ)	10

target response (roughly 200 m).

Using a model antenna pattern, a typical ocean backscatter at  $28^\circ$ , and an expected system noise level, we find that the clutter at 1 km altitude could exceed the system noise by up to 45 dB, seriously limiting sensitivity. If a layer of rain were present, the attenuation at 35 GHz in the rain would reduce the surface clutter. For example, a 5-km thick layer of rain with 10-mm/h rain rate would have a round-trip attenuation of 25 dB, based on Mie scattering calculations. Even so, the surface return would still be 20 dB above the system noise; hence, clutter suppression is needed to enable the NIS concept.

### 3. CLUTTER SUPPRESSION METHOD

To reliably reduce clutter, we consider using Doppler clutter cancellation methods, as have been applied to ground-based weather radar [5]. These methods are not applicable to low-earth orbit precipitation radars because of the large platform motion. However, for NIS the geostationary platform motion (relative to the earth's surface) is expected to be very small, so investigation of these techniques is reasonable. We assume that the mean motion of clutter is zero, with a velocity spread of 1 m/s due to random motions of the ocean surface and spacecraft. The ocean component is expected to dominate; if two-scale scattering theory (e.g., [6]) holds, the Doppler spectrum width should be determined by the wave orbital motions of the long wave spectrum. Measurements indicate that the ocean Doppler width should be less than about 1 m/s [7]. The expected precipitation spectrum has a maximum width of 4 m/s dominated by effects of varying fall velocities, turbulence, cross-beam effects, and non-uniform beam-filling [8, 9].

To simulate the effect of clutter filtering, the output of a mesoscale numerical model for a mesoscale convective system (MCS) is used to generate radar reflectivity and Doppler spectra. The result is placed in a simulated NIS beam, and notch filtering at 0 Hz is performed (with spectral density interpolation). Fig. 1 shows the geometry of the simulation, with the NIS beam intersecting the MCS. Fig. 2 shows a simulated Doppler spectrum versus altitude (clutter is dark red, extending from surface to 3 km altitude, around the zero-Doppler velocity) for  $15^\circ$  incidence. The precipitation spectrum is yellowish and to the right (positive velocity) due to the raindrop fall speed. At higher altitudes the precipitation spectrum extends downward to zero velocity, due to the small vertical motion of snow and ice particles. This scenario is representative of a large majority of cases and indicates that the clutter rejection filter should only be applied to range bins near the surface.

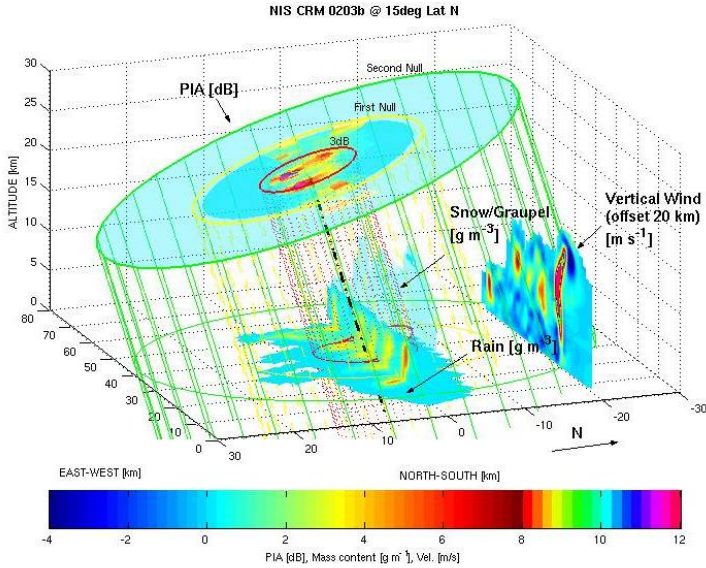


**Figure 1.** Geometry for Doppler clutter cancellation simulation. The NIS beam intersects a simulated mesoscale convective system (MCS).

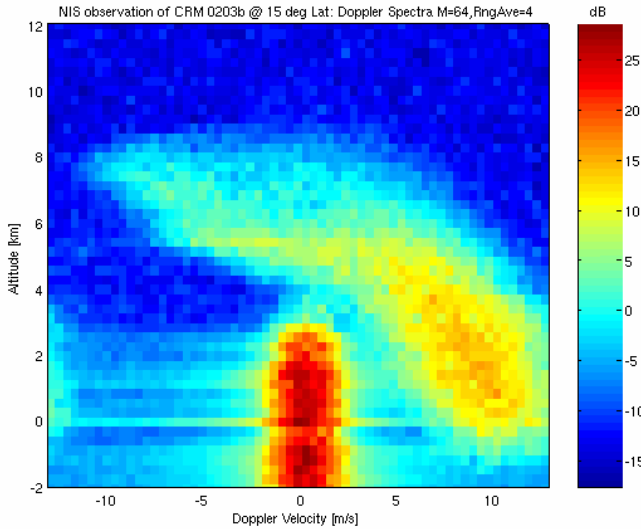


**Figure 2.** Doppler spectrum versus altitude. The strong, red area at lower center is the clutter return, extending to about 3 km altitude.

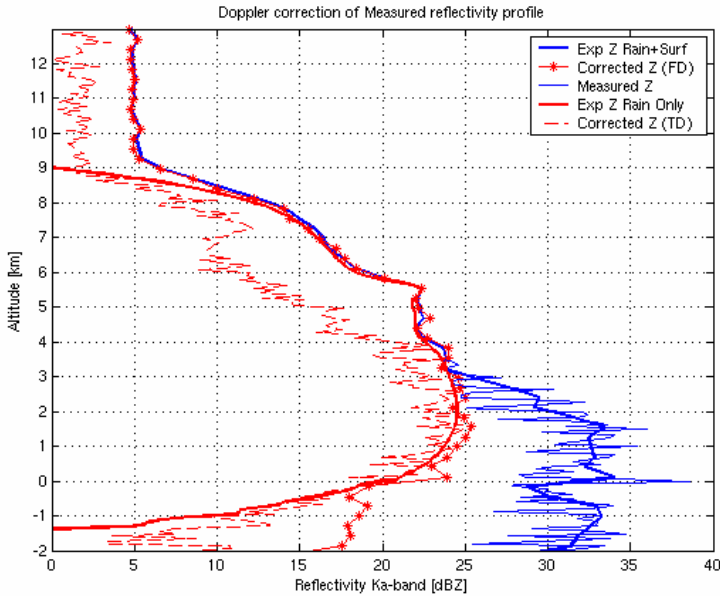


**Figure 3.** Reflectivity  $Z$  versus altitude. Blue solid thick line is the expectation of the measured reflectivity, and blue dashed line includes fading noise. Red solid thick curve is the ‘truth’, i.e., expectation of the rain reflectivity, without surface clutter. Red dashed is notch filtering in time domain (TD) and red with asterisk is notch filtering in frequency domain (FD), with additional processing described in text.

Figure 3 shows radar reflectivity versus altitude. The ‘truth’ profile is the power that would be received from rain and other hydrometeors if no surface were present; it’s the clutter-free rain reflectivity. The observed reflectivity profile would be measured by NIS; it overlaps the ‘truth’ reflectivity profile above 3km, but it includes significant ground clutter contribution in the lower 3km. The simplest approach to remove ground clutter is the application of a ‘notch’ (i.e., bandstop filter around zero Doppler) in the time domain. This approach is extremely effective in removing ground clutter contamination (see red dashed curve versus red solid below 3km), but it also cancels any return from atmospheric targets with small Doppler velocity (see red dashed curve versus red solid above 4km). Since the viewing geometry is known, basic a priori information on the vertical extent of the ground clutter is also known and can be used to filter ground clutter only where ground clutter is possible.

Also, a Gaussian assumption on the spectral characteristics of the rain can mitigate the ‘notching’ of any portion of the rain spectrum that is masked by ground clutter. The effectiveness of this approach relies on the fact that it is unlikely for the rain spectrum to be at the same time centered on the zero-Doppler line and have a spectral width smaller than that of the underlying surface. Application of the knowledge of both clutter location and rain spectral shape is conveniently done in the altitude-frequency domain (e.g., Fig. 2). First, a least mean square Gaussian fit is used with a fixed mean at zero-Doppler and free width and amplitude parameters; the resulting best fit is the surface clutter spectrum  $P_{SC}$  which is removed from the observed spectrum  $P_{OBS}$  (notch filter). All portions of the residual spectrum  $P_R = P_{OBS} - P_{SC}$  where  $P_R > P_{SC}$  are used for a second least mean square Gaussian fit (with all three parameters free). The resulting fit is the estimated rain spectrum, and its integral is the estimated rain contribution to the total reflectivity. The resulting profile of reflectivity (red with asterisk) is similar to the ‘truth’ profile, from the surface (0 km altitude) to the top of the observed profile indicating that the notch filtering has successfully removed clutter. In the example shown, clutter suppression is roughly 15 dB.

#### 4. CLUTTER SUPPRESSION WITH A STAGGERED PRF

Simulations with various model precipitation systems indicate that Doppler filtering as discussed in the previous section can be used to significantly reduce clutter and improve sensitivity close to the surface. However, Doppler filtering is most easily applied to data with a constant pulse repetition frequency (PRF), (i.e., constant  $T$ , the pulse repetition interval PRI, the reciprocal of the PRF). In fact, a staggered PRF is likely needed for NIS to resolve ambiguities [5]. For a uniform PRF of 7 kHz the maximum unambiguous velocity  $\lambda/4T$  is 15 m/s; larger velocities will be folded into this interval and use of aliasing correction algorithms similar to those developed for ground based weather radars would be necessary. Use of larger PRFs is complicated by the need for unambiguously resolving the lower troposphere. For a staggered PRF, where an interval  $T_1$  is followed by an interval  $T_2$ , the maximum unambiguous velocity is  $\lambda/4(T_1 - T_2)$  [5]. The advantage is that the effective period is  $T_1 - T_2$  substantially increasing the maximum unambiguous velocity without reducing the maximum unambiguous range. The disadvantage is that clutter filtering becomes much more challenging.

The problem can be interpreted as inserting zeroes in the time

series to create a new time series with very high sample rate. This has the effect of creating additional clutter images at other frequencies in the spectrum, so that clutter filtering involves removing the clutter at zero and these other frequencies. We can do this by applying notch filters at zero and the other clutter frequencies or we can apply the frequency domain method of Sachidananda and Znic [10, 11] to remove clutter but leave signal. We choose the second approach, since it can be combined with the frequency domain method of the previous section to remove clutter while preserving the rain spectrum. Although the Sachidananda and Znic method was developed for S-band weather radar, it is applicable to our Ka-band radar concept.

Given our desired maximum unambiguous velocity  $v_a$ , the required PRI for a uniform PRF is  $T_u = \lambda/4v_a$ . The PRIs for staggered operation are then derived as integers  $n_1$  and  $n_2$  times  $T_u$ . The received signal at the high rate (after inserting zeros) is a uniform series with spacing  $T_u$  modulated by a train of 1's and 0's. In the frequency domain the measured spectrum is the convolution of the true spectrum with the spectrum of the modulating sequence. The modulating spectrum consists of spikes of varying amplitudes spaced at  $n/(n_1 + n_2)$  frequency bins, where  $n$  is the number of samples at the high rate. This is illustrated in Fig. 4 for the case of  $n_1 = 4$  and

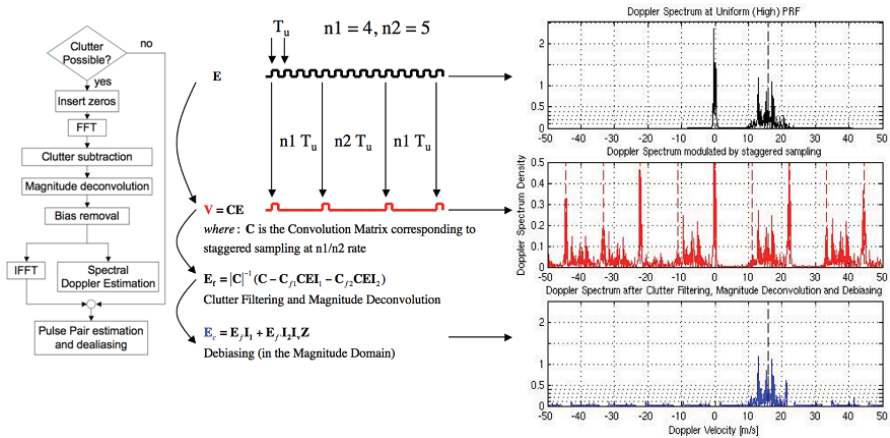


**Figure 4.** Left, flow diagram of the algorithm. Right: illustration of the effects of staggered PRF on the Doppler spectrum. The upper panel is the spectrum  $E$  if data were acquired at  $T_u = 18$  kHz; clutter is narrowband near 0 m/s. The middle panel is the spectrum  $V = CE$ , due to use of a staggered PRF ( $n_1 = 4, n_2 = 5$ ). The lower panel is the rain spectrum recovered using the method of [10] and [11]. Processing steps are described at center.

$n_2 = 5$  and  $T_u$  corresponds to 18 kHz PRF; to the left of the frames are explanations of the steps for generating each frame. The top frame is the spectrum that would be observed if the PRF corresponding to  $T_u$  is used. The spectrum for the staggered PRF sequence is shown in the middle frame; it can be seen that the true spectrum is convolved with a sequence of spikes, giving replicas of the ground clutter at non-zero locations. The staggered PRF signal discrete Fourier Transform (DFT) is  $V = CE$ , where  $C$  is the modulation matrix and  $E$  is the DFT corresponding to the spectrum in the upper frame. The method of Sachidananda and Zrnic [10, 11] reconstructs  $E$  with clutter removed by first subtracting a clutter estimate and then performing a magnitude deconvolution; this is followed by debiasing as shown in the description to the left of the frames. The lower frame shows the spectrum after using the Sachidananda and Zrnic method. In our implementation, the portion of spectrum thus removed is filled with values obtained by interpolating the residual portion of the spectrum. Alternatively the same Gaussian fit approach described in the previous section can be implemented. The resulting spectrum is similar to that for the hypothetical high PRF case; it can be used directly to obtain clutter-free estimates of reflectivity and mean Doppler velocity, or it can be inverse transformed to apply a staggered pulse-pair algorithm for the same purpose [5]. Both approaches were tested in this work and they produce generally comparable results with differences in performance dictated mainly by the specific scenarios and configurations. We tested other values of  $n_1$  and  $n_2$  besides 4 and 5. We found that 4 and 5 provide best results for NIS. Smaller numbers require PRFs that are too large, causing range ambiguities. Large numbers result in estimates that are too noisy, due to the small difference in PRFs.

To further test this approach we performed Monte Carlo experiments with simulated clutter-contaminated precipitation spectra with velocities ranging from  $-50$  to  $+50$  m/s and velocity widths of 1, 2 or 3 m/s. For each mean velocity and velocity width we performed 1000 runs, and for each run, we generated a noisy time series according to the method originally described in [12] and performed frequency domain filtering to recover the velocity from the spectrum resulting from a staggered PRF. The surface clutter spectrum was assumed to be centered on zero-Doppler with a width between 0.35 and 1 m/s. We found 70% of the velocity estimates to be within 1 m/s of the true velocity, while 91% were within 2 m/s. We also found that clutter after filtering is typically well below the signal. When the rain spectrum is at 5 m/s, for example, the clutter can be suppressed to 19 dB below the signal. In general, as expected, the algorithm performance depends mainly on the separation between the surface and the rain spectra:

simulated results show a surface clutter rejection of about 20 dB in case of 2-sigma separation (i.e., the centers of the two spectra are separated by more than twice the sum of their widths), decreasing to about 4 dB for 1-sigma separation. The most challenging scenarios are obviously those where rain and surface spectra are entirely overlapped; in this case useful performance seems achievable only for moderately broad rain spectra (i.e., 2 m/s or more). The main limitation of the method thus occurs when the rain spectrum is both narrow and centered at zero Doppler. Fortunately, this case requires light rain and a wind component of around 5 m/s in the radar look direction; this is an unlikely situation in the severe weather and hurricanes that would be targeted by NIS. Our results indicate that while clutter presents a significant challenge for NIS, Doppler filtering can significantly reduce its effects, even when using a staggered PRF.

## ACKNOWLEDGMENT

This research was carried out at the Jet Propulsion Laboratory, California Institute of Technology, under a contract with the National Aeronautics and Space Administration. Support from the NASA Earth Science Technology Office is appreciated.

## REFERENCES

1. Kozu, T., T. Kawanishi, H. Kuroiwa, M. Kojima, K. Oikawa, H. Kumagai, K. Okamoto, M. Okumura, H. Nakatsuka, and K. Nishikawa, "Development of Precipitation Radar onboard the Tropical Rainfall Measuring Mission (TRMM) satellite," *IEEE Trans. Geosci. Remote Sensing*, Vol. 39, 102–116, 2001.
2. Tanelli, S., S. L. Durden, E. Im, K. Pak, D. Reinke, P. Partain, J. Haynes, and R. Marchand, "CloudSat's Cloud Profiling Radar after two years in orbit: Performance, external calibration, and processing," *IEEE Trans. Geosci. Remote Sensing*, Vol. 46, 3560–3573, 2008.
3. Im, E., E. A. Smith, S. L. Durden, S. Tanelli, J. Huang, Y. Rahmat-Samii, and M. Lou, "Instrument concept of NEXRAD In Space (NIS) – A geostationary radar for hurricane studies," *Proc. Int. Geosci. Remote Sens. Symp.*, 2003.
4. Bahadori, K. and Y. Rahmat-Samii, "An array-compensated spherical reflector antenna for a very large number of scanned beams," *IEEE Trans. Antennas Propagat.*, Vol. 53, 3547–3555, 2005.

5. Doviak, R. J. and D. S. Zrnic, *Doppler Radar and Weather Observations*, 2nd Edition, Academic Press, San Diego, 1993.
6. Wu, Z.-S., J.-P. Zhang, and L.-X. Guo. "An improved two-scale model with volume scattering for the dynamic ocean surface," *Progress In Electromagnetics Research*, PIER 89, 39–56, 2009.
7. Plant, W. J. and W. C. Keller, "Evidence of Bragg scattering in microwave Doppler spectra of sea return," *J. Geophys. Res.*, Vol. 95, 16299–16310, 1990.
8. Meneghini, R. and T. Kozu, *Spaceborne Weather Radar*, Artech House, Boston, MA, 1990.
9. Amayenc, P., "Proposal for a spaceborne dual-beam rain radar with Doppler capability," *J. Atmos. Oceanic Technol.*, Vol. 10, 262–276, 1993.
10. Sachidananda, M., and D. S. Zrnic, "Clutter filtering and spectral moment estimation for Doppler weather radars using staggered pulse repetition time (PRT)," *J. Atmos. Oceanic Technol.*, Vol. 17, 323–331, 2000.
11. Sachidananda, M., and D. S. Zrnic, "An improved clutter filtering and spectral moment estimation algorithm for staggered PRT sequences," *J. Atmos. Oceanic Technol.*, Vol. 19, 2009–2019, 2002.
12. Zrnic, D. S., "Simulation of weatherlike Doppler spectra and signals," *J. App. Meteor.*, Vol. 14, 619–620, 1975.